ELSEVIER

Catalysis Today 47 (1999) 263–277

CATALYSIS TODAY

Unsteady state treatment of very lean waste gases in a network of catalytic burners

M. Brinkmann, A.A. Barresi*, M. Vanni, G. Baldi

Dipartimento di Scienza dei Materiali e Ingegneria Chimica, Politecnico di Torino, Corso Duca degli Abruzzi 24, 10129 Torino, Italy

Abstract

Catalytic reactors in forced non-stationary operation enable autothermal VOC oxidation even at extremely low adiabatic temperature rise. A network of three reactors in series with large inert sections is presented as an alternative to the reverse-flow reactor.

A one-dimensional model for simulation of VOC oxidation in forced non-steady state packed bed catalytic reactors has been developed and implemented into a program that uses standard mathematical software. Numerical simulation reveals that the network of three catalytic reactors in series with large inert sections is a suitable design for VOC oxidation at low concentration. The system can be controlled by a simple set of two switches acting according to temperature setpoints.

Maximum temperature is very sensitive to heat transfer, which cannot be considered as infinitely fast despite small temperature gradients between gas and solid. These dependencies are somewhat less pronounced at higher load.

Keywords: Non-stationary burners; Reactor network; Waste gases; Catalytic combustor

1. Introduction

During the last decades, air pollution control mainly covered the fields of dust removal, absorption of gases such as sulphur dioxide or nitrogen oxides and others. Technical demands of industrial gas cleaning as well as environmental legislation following public awareness led to substantial reduction of emissions. More recently, volatile hydrocarbons or VOCs (volatile organic compounds) have been found to play a key role in the formation of photochemical smog. It has therefore become necessary to avoid or, where impossible, to remove even low concentrated VOC emissions.

In contrast to highly loaded gas streams, it is not economical to recover the VOCs from low concentration waste gases or from complex mixtures thereof. In these cases, destructive methods such as biofiltration or thermal incineration are preferred. The latter may be performed by an open flame or by means of suitable catalysts. Catalytic combustion requires a certain temperature of the catalyst bed, which is provided by the gas stream itself or by external heating. In both cases, large amounts of energy are spent in maintaining reaction temperature.

Therefore it is a usual practice to use the (exothermic) heat of reaction to preheat the cold inlet gas stream in a heat exchanger, that may be designed as a

*Corresponding author. Tel.: +39-011-5644658; fax: +39-011-5644699; e-mail: barresi@athena.polito.it

0920-5861/99/$ – see front matter
PII: S0920-5861(98)00307-1

separate device or as part of the catalytic reactor itself. Balmer and Gilles [1] as well as Eigenberger and Nieken [2] present some technical solutions. However, for very low combustible load the heat exchange section takes unreasonable dimensions.

These difficulties can be overcome by using apparatuses for continuous yet forced non-stationary operation. One example is the reverse-flow reactor developed by Boreskov and Matros [3,4]. This design has also been investigated by other authors with respect to modelling and applications, which have been proposed, e.g. in the fields of SO_2 oxidation, ammonia synthesis and methanol production [5]. The aspects of VOC oxidation and catalytic combustion have been treated especially by Nieken et al. [6], Matros et al. [7], Chaouki et al. [8], van de Beld et al. [9], and Züfle et al. [10,11].

The system consists of a catalytic reactor and a set of valves at the inlet and outlet so that the gas flow direction can be reversed. The cold inlet gas is heated by the solid, creating a slowly moving temperature front. Whereas a stationary system would suffer a "quench-off" due to cooling down the catalyst, switching the flow direction maintains reaction temperature inside the catalyst bed. Both ends of the reactor thus act as heat exchangers and may be replaced by inert material as suggested by several authors [2,4,9,12,13]. The apparatus is operated in forced non-stationary conditions; however, a periodic state is reached after typically 100–200 switches [14]. This periodic state is characterized by identical temperature profiles at the beginning of each cycle, and by constant time-average conversion. Therefore it is also referred to as pseudo-steady-state.

The drawback of this design is the relative high switching frequency, which requires high quality valves. Furthermore, washout of fully contaminated gas occurs at the beginning of each cycle. Balmer and Gilles [1] as well as Eigenberger and Nieken [2] present valveless solutions which are based on the same idea of creating moving temperature fronts inside catalytic reactors. Matros [4] also suggests a network of two catalytic reactors in series, with constant flow direction and the heat front propagating in a closed circle. This is achieved on changing the order of reactors by a set of valves. Unfortunately, little is known about performance and behaviour of this design.

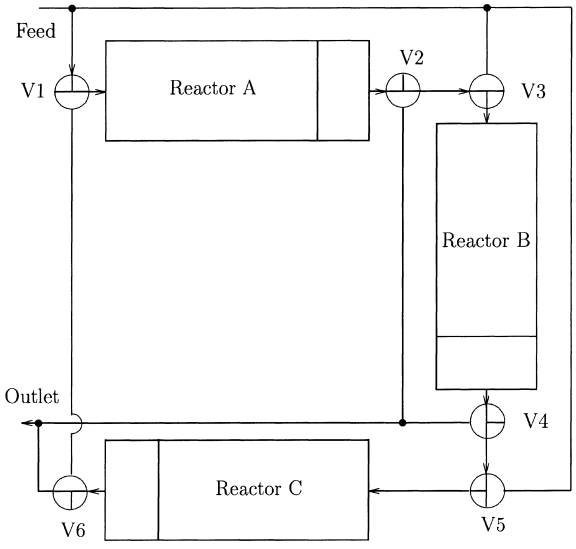

Fig. 1. Scheme of three reactors in series with variable feed position.

In this work we consider a network of three reactors in series as depicted in Fig. 1. Three reactors have been chosen as this configuration should be more reliable than that with only two combustors: it is thought to be more stable and strongly reduces the spot emissions of unburned waste in correspondence of switching. Each reactor consists of a large inert section for heat exchange and a relatively small catalytically active part near the outlet; a 3 m long reactor with 20% active part has been generally considered. A set of valves enables us to vary the feed position, thus changing the sequence of reactors. For example, switching the valves V1–V3 and V6 of Fig. 1 will change the reactor sequence from A-B-C to B-C-A. Contrary to the reverse-flow reactor, the flow direction is maintained in this way. Various switching criteria are discussed in Section 3.1.

It will be shown by means of numerical simulation that the proposed design is capable of treating gas streams even of extremely low combustible load, with good conversion and without further need of energy. A two-point control strategy will be adopted. A parametric sensitivity study will be conducted to point out the effects of transport parameters on conversion and maximum temperature; the influence of the design variables will also be investigated.

2. The model

A heterogeneous mathematical model has been developed in order to investigate the performance of the network of packed bed reactors. The adiabatic, one-dimensional model features dispersive transport of energy and mass in the gas phase. In this way second order derivatives are included in the model equations. Solid bed conductivity has not been considered in the model equations, but the effect has been included in the axial heat dispersion coefficient, by considering an effective gas conductivity. It is assumed that no accumulation of mass occurs near the solid surface, where the combustible reacts according to a first order law. Pressure loss inside the reactor is neglected, and heat capacity is assumed to be constant. The balance equations for the catalytically active sections thus write:

$$\rho\frac{\partial T_G}{\partial t} = -v\rho\frac{\partial T_G}{\partial x} + \frac{k_{eff}}{c_P}\frac{\partial^2 T_G}{\partial x^2} + \frac{h_t a}{c_P \epsilon}(T_S - T_G), \quad (1)$$

$$\frac{\partial T_S}{\partial t} = \frac{k_G a(-\Delta H)}{\rho_S c_{P,S}(1-\epsilon)}(c_G - c_S) - \frac{h_t a}{\rho_S c_{P,S}(1-\epsilon)}(T_S - T_G), \quad (2)$$

$$\frac{\partial(\rho y_G)}{\partial t} = -\frac{\partial(v\rho y_G)}{\partial x} + D_{eff}\frac{\partial^2(\rho y_G)}{\partial x^2} - \frac{k_G a}{\epsilon}\rho(y_G - y_S), \quad (3)$$

$$0 = \frac{k_G a}{M}\rho(y_G - y_S) - r. \quad (4)$$

A first order kinetic law with respect to the combustible and independent from the oxygen concentration has been considered:

$$r = k_1 c_S. \quad (5)$$

The kinetics of VOC combustion in excess oxygen can be well described by this kinetic law in many cases; this same law has been adopted by other researchers [7,14,15]. In this work the kinetic parameters determined by van de Beld [14] for ethene combustion have been considered: $k'_\infty = 0.18\,\mathrm{mol\ kg_{cat}^{-1}\,s^{-1}\,Pa^{-1}}$; $E'_A = 57800\,\mathrm{J\,mol^{-1}}$. In this case Eq. (4) can be solved for y_S:

$$y_S = \frac{1}{1 + k_1/k_G a} y_G. \quad (6)$$

Substituting Eq. (6) into Eqs. (2) and (3), a system of three coupled, nonlinear, parabolic partial differential equations is obtained. For computational purposes it is better to use the dimensionless form:

$$\frac{\rho}{\rho_0}\frac{\partial \tau_G}{\partial s} = -\frac{\partial \tau_G}{\partial z} + \frac{1}{\mathrm{Bo}_H}\frac{\partial^2 \tau_G}{\partial z^2} + \mathrm{St}_H(\tau_S - \tau_G), \quad (7)$$

$$\frac{\partial \tau_S}{\partial s} = \frac{\mathrm{St}_M \Delta T_{ad}}{(CR)T_0}\frac{\rho}{\rho_0}Y_G\left(1 - \frac{1}{1+\mathrm{Ha}}\right) - \frac{\mathrm{St}_H}{CR}(\tau_S - \tau_G), \quad (8)$$

$$\frac{\rho}{\rho_0}\frac{\partial(Y_G)}{\partial s} = -\frac{\partial Y_G}{\partial z} + \frac{1}{\mathrm{Bo}_M}\frac{\partial^2}{\partial z^2}\left(\frac{\rho}{\rho_0}Y_G\right) - \mathrm{St}_M\frac{\rho}{\rho_0}(Y_G - Y_S), \quad (9)$$

with:

$$z = x/L, \quad s = tv_0/L, \quad \Delta T_{ad} = \frac{y_G^f(-\Delta H)}{c_{P,G}M},$$

$$\tau_G = T_G/T_0, \quad \tau_S = T_S/T_0, \quad Y_G = y_G/y_G^f,$$

$$\frac{1}{\mathrm{Bo}_H} = \frac{k_{eff}}{c_P L v_0 \rho_0}, \quad \frac{1}{\mathrm{Bo}_M} = \frac{D_{eff}}{Lv_0}, \quad CR = \frac{(1-\epsilon)\rho_S c_{P,S}}{\epsilon\rho_0 c_{P,G}},$$

$$\mathrm{St}_H = \frac{h_t a L}{c_{P,G}\epsilon v_0 \rho_0}, \quad \mathrm{St}_M = \frac{k_G a L}{\epsilon v_0}, \quad B = -E_A/(RT_0),$$

$$\mathrm{Ha} = \mathrm{Ha}_0 \exp(-B/\tau_S), \quad \mathrm{Ha}_0 = k_\infty/(k_G a).$$

For the gas phase, Danckwerts boundary conditions are assumed, giving:

$$-1/\mathrm{Bo}_H\frac{\partial \tau_G}{\partial z} = 1 - \tau_G, \quad (10)$$

$$-\frac{\rho}{\rho_0}1/\mathrm{Bo}_M\frac{\partial Y_G}{\partial z} = 1 - Y_G \quad (11)$$

at z=0, and

$$\frac{\partial \tau_G}{\partial z} = 0, \quad (12)$$

$$\frac{\partial Y_G}{\partial z} = 0 \quad (13)$$

at z=1.

In the inert section no mass transfer and reaction occur, and consequently there is no heat generation. Thus in the region the balance equations simplify to:

$$\frac{\rho}{\rho_0}\frac{\partial \tau_G}{\partial s} = -\frac{\partial \tau_G}{\partial x} + \frac{1}{\mathrm{Bo}_H}\frac{\partial^2 \tau_G}{\partial z^2} + \mathrm{St}_H(\tau_S - \tau_G), \quad (14)$$

$$\frac{\partial \tau_S}{\partial s} = -\frac{\mathrm{St}_H}{CR}(\tau_S - \tau_G), \quad (15)$$

$$\frac{\rho}{\rho_0}\frac{\partial(Y_G)}{\partial s} = -\frac{\partial Y_G}{\partial z} + \frac{1}{Bo_M}\frac{\partial^2}{\partial z^2}\left(\frac{\rho}{\rho_0}Y_G\right). \quad (16)$$

The parameters for dispersion and transfer of energy and mass are either fixed values (for sensitivity analysis), or, in some cases, are calculated from the literature correlations suggested by van de Beld [14].

Concerning axial dispersion of mass, a correlation having the following form:

$$\frac{D_{eff}}{v_0 d_P} = \frac{\alpha_1}{Re_P\,Sc} + \frac{\alpha_2}{1+\alpha_3/(Re_P\,Sc)} \quad (17)$$

has been considered, where α_1=0.73, α_2=0.5 and α_3=9.7 according to Edwards and Richardson [16].

A similar correlation, in the form proposed by van de Beld [14], is employed for evaluating the effective axial heat dispersion coefficient:

$$\frac{k_{eff}}{(\rho c_{P,G})_0 v_0 d_P} = \frac{\alpha_1 + \lambda_{st}/\lambda_G}{Re_P\,Pr} + \frac{\alpha_2}{1+\alpha_3/(Re_P\,Pr)}. \quad (18)$$

The stagnant contribution λ_{st}/λ_G is calculated from the Zehner–Bauer equations [17].

For the gas–solid heat transfer coefficient the equation proposed by Gnielinski [18] is adopted:

$$j_h = \frac{1.6[2 + F(Re/\epsilon)^{0.5}Pr^{1/3}]}{Re\,Pr^{1/3}}, \quad (19)$$

with

$$F = 0.664\sqrt{1+\left(\frac{0.0557(Re/\epsilon)^{0.3}Pr^{2/3}}{1+2.44(Pr^{2/3}-1)(Re/\epsilon)^{-0.1}}\right)^2}. \quad (20)$$

However, the choice of correlation is not crucial for Re>20, which is given at reasonable operation conditions. Analogy between heat and mass transfer is assumed in order to evaluate the mass transfer coefficients.

A simplified model can be proposed for infinitely fast heat transfer, i.e. T_G=T_S. The remaining pseudo-homogeneous energy balance is obtained from addition of Eqs. (1) and (2), and in dimensionless form

$$\left(\frac{1}{\tau}+CR\right)\frac{\partial\tau}{\partial s} = -\frac{\partial\tau}{\partial z} + \left(\frac{1}{Bo_H}+\frac{CR}{Bo_S}\right)\frac{\partial^2\tau}{\partial z^2} + St_M\Delta T_{ad}\frac{1}{\tau}Y_G\left(1-\frac{1}{1+Ha}\right) \quad (21)$$

is obtained. The mass balance equation and boundary conditions remain the same. The applicability of this simplified model will be discussed in Section 4.

A two-point control policy is adopted, in order to switch the feeding point assuring stable operating conditions. The details are given in the following.

For simulation purposes the whole system is assumed to be continuous in order to reduce the number of variables and to spare computer memory. The parabolic PDE system is solved by the Fortran-Routine D03PCF of the NAG-Library Mk15. This solver is based on spatial discretization (101 mesh points per reactor) and an ODE-solver that uses Gear's method. Time-average outlet temperature and conversion are obtained from the integration routine D01GAF (also NAG-Library). When the switching condition is fulfilled, the current solution is shifted with respect to space variable and taken as initial condition for the next period.

3. Results

3.1. Startup and pseudo-steady-state

For the goal of autothermal operation it is necessary to heat up the catalytic reactors to a certain temperature prior to feeding the cold waste gas. Indeed, technical combustors are often equipped with gas burners or electrical heating devices to preheat gas and reactor solid material. In the simulations it is assumed that the reactor is initially at uniform temperature of about 530 K, with zero concentration of combustible. The calculations have been carried out with non-constant transport parameters and with system properties as defined in Table 1.

On feeding the cold waste gas, the combustible reaches the first catalytic section in less than one residence time due to thermal expansion of the gas phase. Thus, after less than three residence times after startup, a concentration profile is established throughout the network. It is flat in the inactive sections and decreasing according to catalyst temperature and kinetics in the active parts.

The cold gas entering the reactor cools down the reactor solid while being heated up itself. The heat transfer coefficient is usually high enough so that gas and solid temperature do not differ by more than about

Table 1
Parameter list for simulations with variable transport parameters

d_R (m)	0.2
L (m)	3.0
d_P (m)	0.006
ϵ	0.4
λ_S (J m^{-2} s^{-1} K^{-1})	0.18
ρ_S (kg m^{-3})	2220
$c_{P,S}$ (J kg^{-1} K^{-1})	1000
P_{act} (%)	20
k'_∞ (s^{-1})	0.18
E'_A (J mol^{-1})	57 800
$-\Delta H$ (J mol^{-1})	1 323 000
p (N m^{-2})	100 000
T_0 (K)	293
M (kg mol^{-1})	0.029
u_0 (m s^{-1})	0.4
$c_{P,G}$ (J kg^{-1} K^{-1})	1373
Y^f_G	0.0003

3 K, but it will be shown later that assuming infinitely fast heat transfer leads to erroneous results.

In this way a temperature front moving in gas flow direction as depicted in Fig. 2 is created. Its velocity depends on gas velocity and capacity ratio as defined in Section 2. Since the volume-based heat capacity of solid is about three orders of magnitude larger than that of gas, the temperature front velocity is very small as compared to gas velocity; the active portion of the first reactor (z=0.8) is reached by the heat front after 1500 residence times.

In the catalytically active parts of the reactors, temperature increases due to the exothermic reaction. This increase is naturally highest in the first (hot) active section where combustible concentration is still large. However, temperature increase is limited by the adiabatic temperature rise ΔT_{ad}. Provided a sufficiently long time, also the following reactor is partially heated up by reaction energy. This occurs approximately for s>1000 in this example. If no control action is taken, the temperature front will pass through the first active zone, cooling down the catalyst below ignition temperature. Reaction is stopped and unburnt combustible enters the second, still hot reactor (Fig. 3, s>1500). However, this is an undesired situation, since part of the catalyst is not in use. At this point it is necessary to introduce some kind of automatic control in order to avoid a switch-off of the whole system.

Different control policies have been considered: the one that gives the best performance is a two-point temperature control [19]. The first temperature control is at the beginning of the first catalytic bed, while the second temperature measurement is located at the beginning of the second catalyst bed; the feed position is changed only if the local temperature drops below setpoint 1 and is above setpoint 2. $T_{SW,1}$=530 K and $T_{SW,2}$=535 K have been chosen. The choice of the setpoints has no significant effect on the cycle time; only the steepness of the profiles increases with setpoints.

The first setpoint is relevant only during startup. By the seventh cycle (more generally, before the tenth), the switch condition in the second section takes over

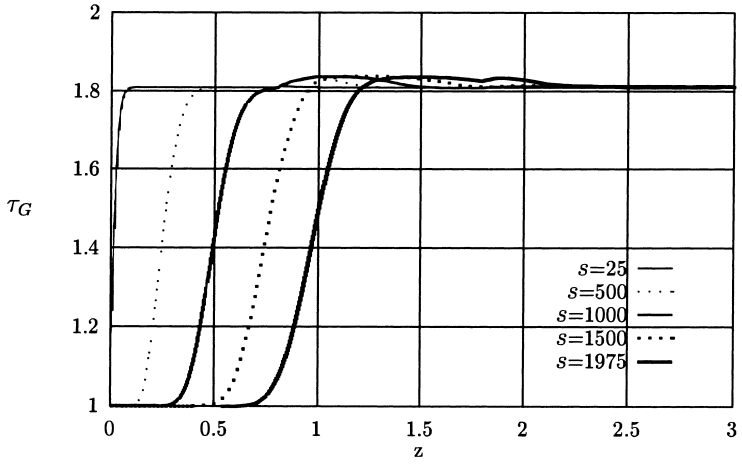

Fig. 2. Moving heat front during the first period.

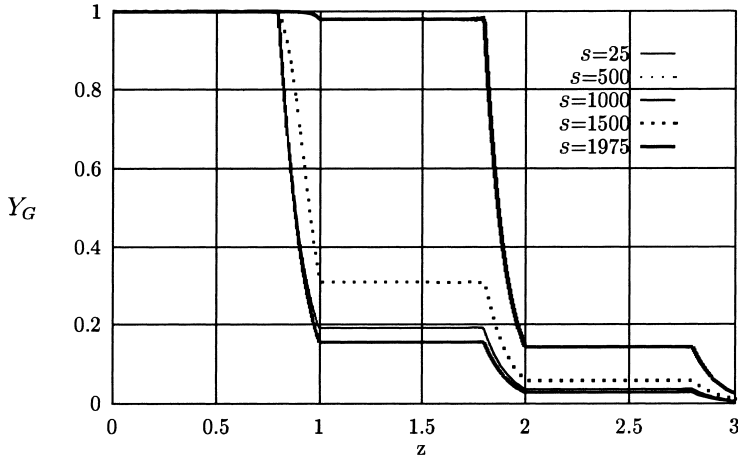

Fig. 3. Concentration profiles during the first period.

control, and the final period duration is already established. In contrast to this, conversion and maximum temperature take much longer to reach their final values, namely 50–100 cycles. Finally, a periodic state of operation is attained that is characterized by the temperature profile moving through the system as shown in Fig. 4. According to temperature, combustion initially occurs mainly in the first, then in the second reactor. Emission of combustible and energy loss in terms of outlet temperature during the stable period are shown in Fig. 5, with time-averaged values as dotted lines. The adopted strategy enables stable autothermal operation even at low combustible load, provided a reasonable choice of setpoints.

3.2. *Influence of operating parameters on performance and light-off*

With the control strategy as described above, autothermal operation is possible with an adiabatic temperature rise of 10 K and conversion higher than 60%. However, a reduced load or different transport parameters may impair stable operation. If the peak temperature drops below the second controllers setpoint, no control action is taken and the cold waste gas cools down also the rest of the reactor. In the following, this process is referred to as ''light-off''. Fig. 6 shows an example of the temperature profiles in case of light-off resulting from slow mass transfer.

It will be shown that there are several mechanisms which affect the peak temperature. If the load is too low or mass transfer is too slow, heat recovery by reaction cannot compensate for energy release in the exit gas stream. Non-adiabacity induces additional heat loss. Strong axial dispersion as well as long catalyst beds flatten the temperature profile, reducing time–space average conversion in extreme cases to light-off.

The effect of mass flow (or inlet flow velocity) is a delicate question since it determines not only the residence time, but also the Reynolds number and thus all transport parameters. Therefore, simulations have been performed on the basis of calculated transport parameters in order to include all interactions. Fig. 7 shows that conversion is much higher at low flow velocity since residence time is large and the attainable maximum temperature is much higher than at higher flow velocity. However, conversion is limited by mass and heat transfer which decrease at reduced mass flow.

The load of combustible, or more precisely the adiabatic temperature rise, is crucial for autothermic operation of the reactor network. This is shown in Fig. 8. For conditions given in Table 1, the minimum adiabatic temperature rise is 10 K. Below this value, light-off occurs. On the other hand, at ΔT_{ad}=20 K, conversion reaches 90% and converges to 98% already at ΔT_{ad}>40 K. Again, maximum temperature dramatically increases with load.

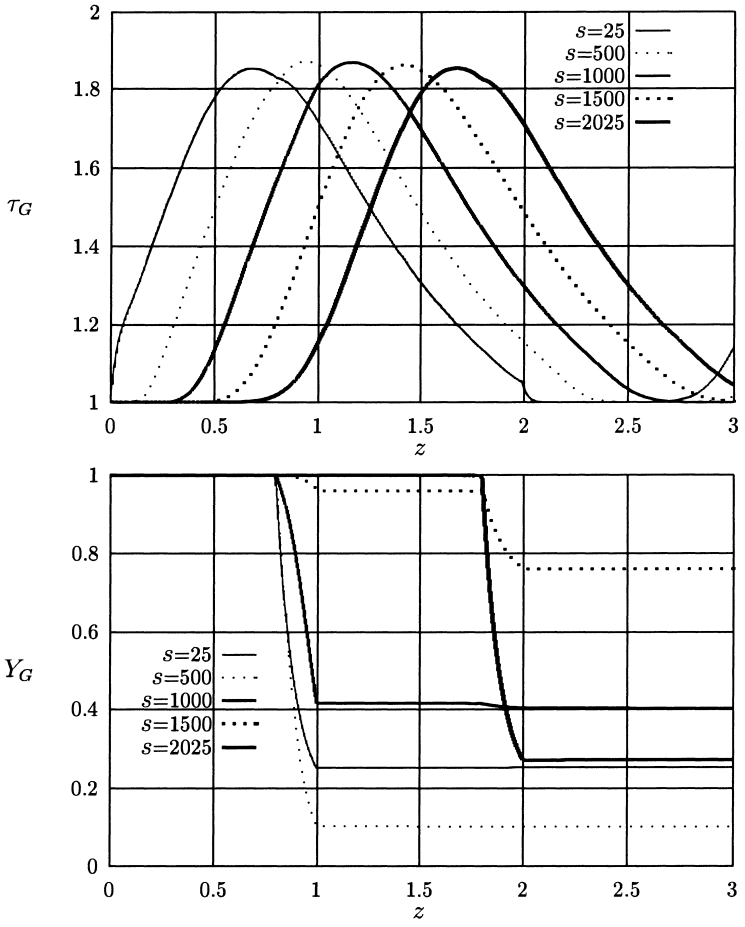

Fig. 4. Moving temperature front and concentration profiles under periodically stable conditions; normalized cycle time n is 2025, corresponding to 6075 s.

3.3. *Effect of design variables*

As expected, conversion increases as the catalytic active portion is increased at the expense of the heat transfer section (Fig. 9, curve a). If the length of the inactive section is kept constant while enlarging the active part, this effect is even more pronounced (curve b). Finally, increasing both sections by the same percentage (i.e. increasing the residence time) leads to the best improvement of conversion (curve c). Note that also the maximum temperature increases especially in case of curve c. This shows that it is not just the total amount of catalyst that determines conversion, but a reasonable combination of residence time and relative amount of active material.

An alternative approach to the suggested network is to "dilute" the catalyst with inert material, thus forming a larger reactive zone with reduced activity. At ΔT_{ad}=10 K, light-off appears as equal portions of catalyst and inert are "mixed". However, higher combustible loads may be treated this way avoiding exceedingly high temperatures.

4. Sensitivity analysis

Optimal choice of operating conditions requires exact knowledge on the influence of transport phenomena such as dispersion, etc. For this reason, a sensitivity analysis has been performed, investigating

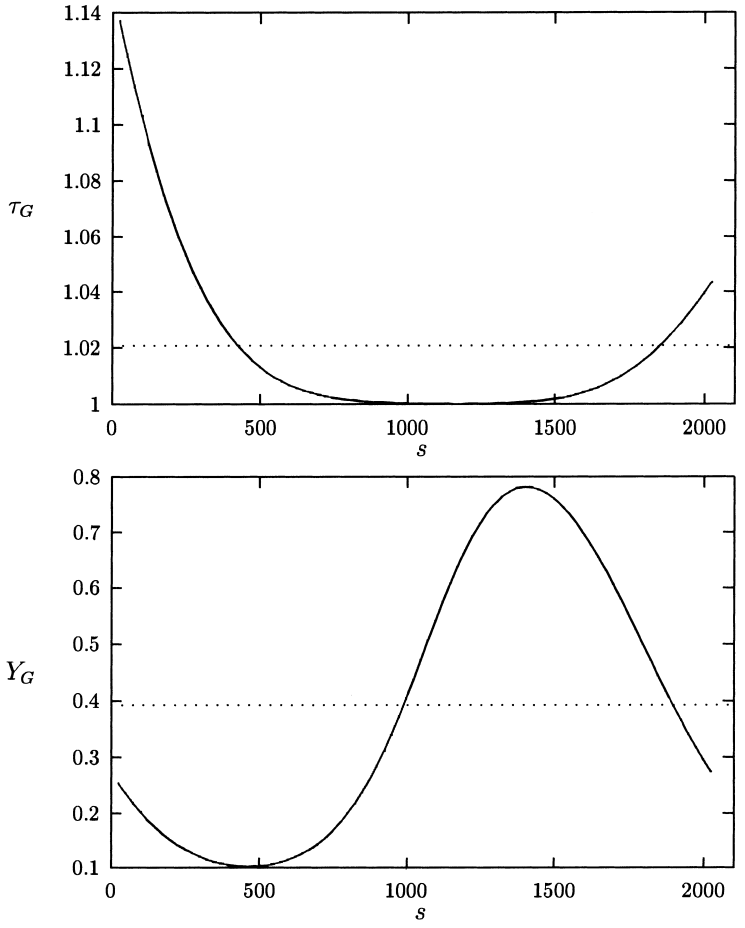

Fig. 5. Exit temperature and concentration under periodically stable conditions.

the effect of transport parameters, capacity ratio, and kinetics on conversion and maximum temperature inside the reactors. The results are shown in Fig. 10. The centre point represents a typical point of operation, evaluated for constant parameters listed in Table 2. These values are obtained from the correlations reported in Section 2 for operation parameters listed in Table 1 and a temperature of 500 K. The error due to assuming constant parameters is small at low adiabatic temperature rise [14], and indeed the results do not differ too much from those obtained with parameters reevaluated in each point.

Starting from the centre point, each parameter is varied by multiples of two. Outlet normalized con-

Table 2
Fixed parameter values at centre point adopted for sensitivity analysis

$1/\mathrm{Bo}_H$	0.001
$1/\mathrm{Bo}_M$	0.0017
St_M	225
St_H	138
ΔT_{ad} (K)	10/30
CR	2038
Ha_0	8
B	6952
T_0 (K)	293
P_{act} (%)	20

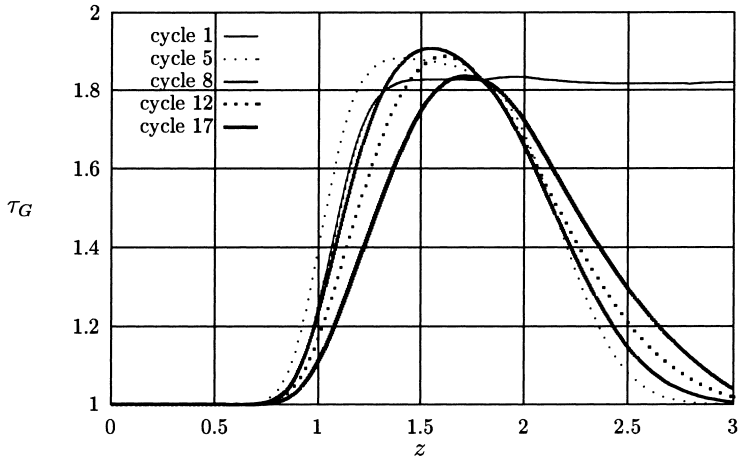

Fig. 6. Temperature profiles at the end of the cycle during light-off due to slow mass transfer; cycle time varies with cycle number, especially at the beginning and slightly towards light-off.

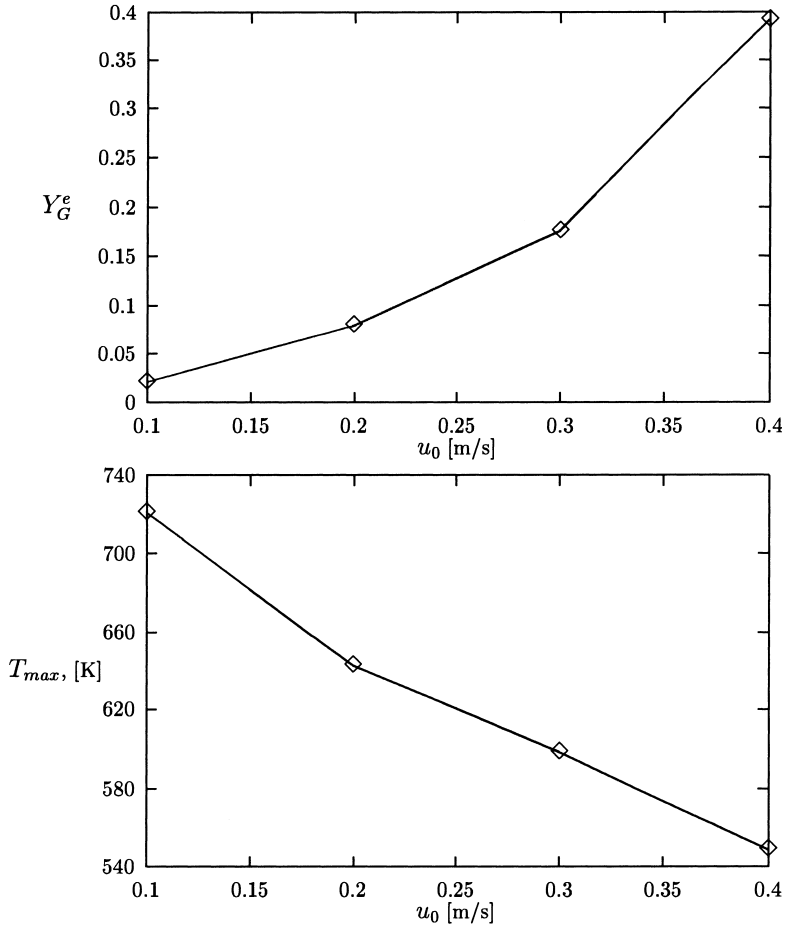

Fig. 7. Influence of flow velocity on exit concentration and maximum temperature (evaluated with variable transport parameters).

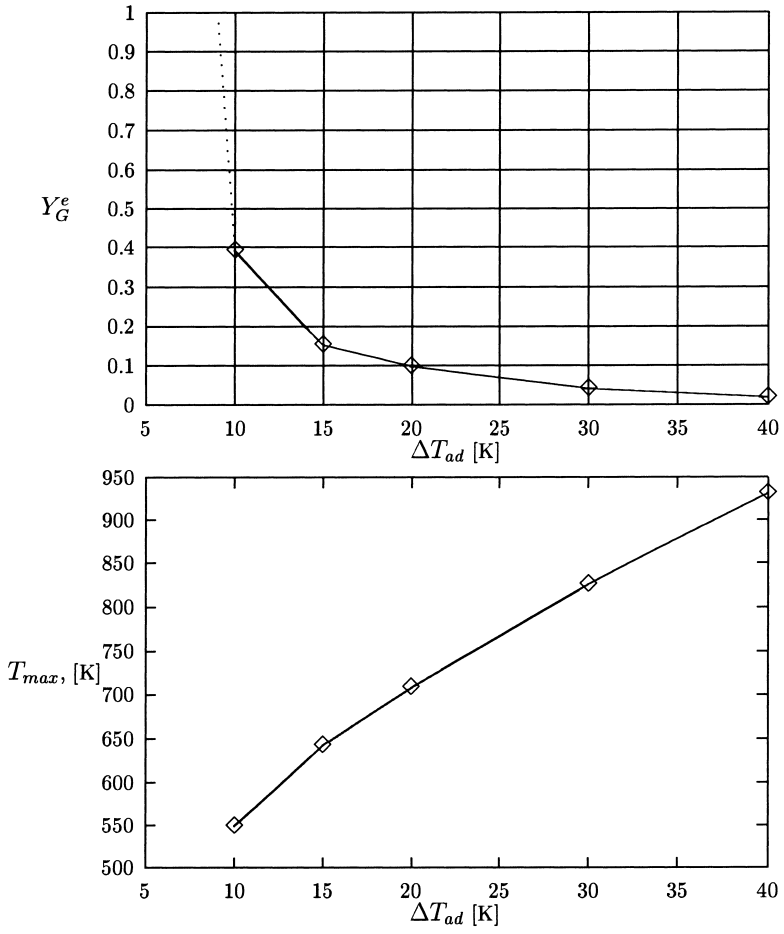

Fig. 8. Influence of combustible load on outlet concentration and maximum temperature (evaluated with variable transport parameters).

centration and $T_{\max}$ are plotted as obtained after 100 switches, when pseudo-steady-state is reached.

As expected, an increased dispersion coefficient of mass slightly decreases conversion since the concentration profiles become less steep. The maximum temperature is almost independent of $1/\mathrm{Bo}_M$. In contrast to this, the axial dispersion rate of energy determines the steepness of temperature profiles and thus of $T_{\max}$. The latter is highest at low dispersion rates. Increased energy dispersion leads to flat profiles and lower reaction temperatures, so that reaction is not maintained any more and light-off occurs. Dispersion of mass and energy are not independent of each other, but the effect of energy dispersion is much more pronounced. However, a low rate of dispersion appears to be desirable.

For the kinetics under consideration and the other parameters in Table 2, the mass transfer parameter St_M is of utmost importance, as is the reaction rate expressed in terms of Ha_0. Increasing St_M by a factor of 4 improves conversion from 63% to 97%, a factor of 8 to more than 99%. This is accompanied by a modest increase in $T_{\max}$. On the other hand, a smaller St_M results in too slow mass transfer and light-off after few switches.

A similar effect on conversion is observed for St_H, the heat transfer parameter, even if it is not as pronounced. But in contrast to the previous one, this parameter has a huge effect on the maximum temperature that determines conversion in this instance. Also, pseudo-steady-state with respect to $T_{\max}$ is obtained much later than after 100 switches if St_H

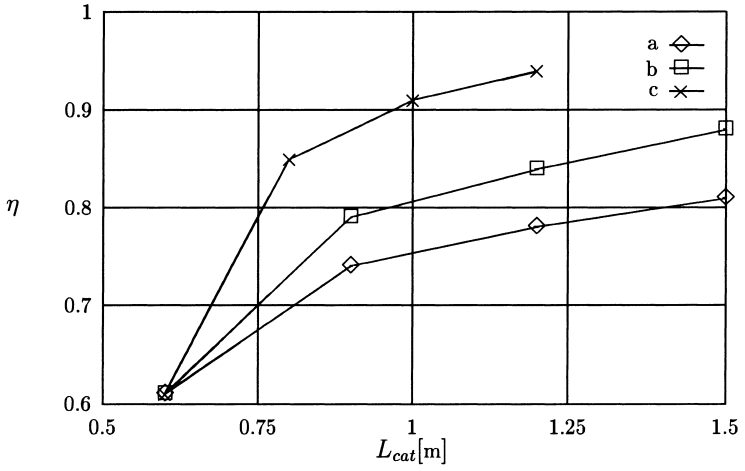

Fig. 9. Effect of catalytic bed length on conversion, in case of an increase of the active portion with fixed total length (curve a), increase of the active part length with constant inert section (curve b) and increase of both sections keeping constant the length ratio (curve c), evaluated with variable transport parameters.

is increased. Fig. 11 shows how T_{max} converges into the value predicted by the simplified model that corresponds to a situation of $St_H \rightarrow \infty$. Note that despite low temperature differences of 1 or 2 K between gas and solid phase, the value of St_H=138 (centrepoint in Fig. 10) cannot be considered to be close to infinity. This indicates that the simplified model is not suitable to describe the situation for parameters given in Table 2, and it explains the diverging yet self-consistent predictions of the different models as sketched in Fig. 12.

In gas–solid reactions, the capacity ratio is a system parameter that cannot be influenced within a wide range. It affects strongly neither T_{max} nor conversion, but determines the heat front velocity, and thus the switching period, almost linearly. Transport parameters, kinetics or load, do not influence dimensionless cycle time.

The observations made at ΔT_{ad}=10 K also hold at a higher load of ΔT_{ad}=30 K. Conversion as well as maximum temperature are generally higher than with lower adiabatic temperature rise, and the sensitivity itself is somewhat lower (if all the other parameters are the same), as shown in Fig. 13.

As expected, an increase in the catalytic active portion yields higher conversion. The influence of the catalytic fraction on sensitivity is shown in Fig. 14; only the effect of St_M, which has been shown to be one of the most relevant parameters, has been analysed. With increasing St_M, conversion is limited by other parameters and cannot be significantly improved by the relative catalyst portion. It is interesting to note that the maximum temperature is reduced if the amount of catalyst is increased.

5. Conclusions

Catalytic reactors in forced non-stationary operation enable autothermal VOC oxidation even at extremely low adiabatic temperature rise. A network of three reactors in series with large inert sections is presented as an alternative to the reverse-flow reactor.

A one-dimensional model for simulation of VOC oxidation in forced non-steady state packed bed catalytic reactors has been developed and implemented into a program that uses standard mathematical software. The model equations consider axial dispersion of heat and mass and a first order reaction at the catalyst surface. Pressure drop is neglected.

Numerical simulation reveals that the network of three catalytic reactors in series with large inert sections is a suitable design for VOC oxidation at low concentration. The system can be controlled by a simple set of two switches acting according to temperature setpoints. This strategy serves for startup and is stable with respect to fluctuating inlet

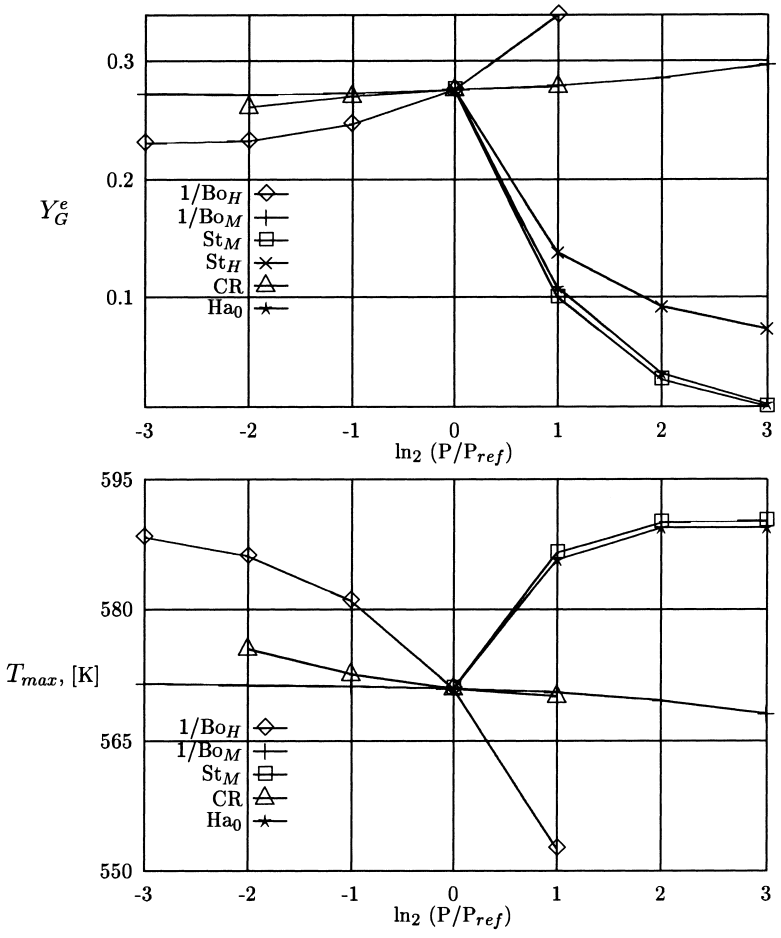

Fig. 10. Dependence of residual concentration and maximum temperature on transport parameters (P) and kinetics; ΔT_{ad}=10 K.

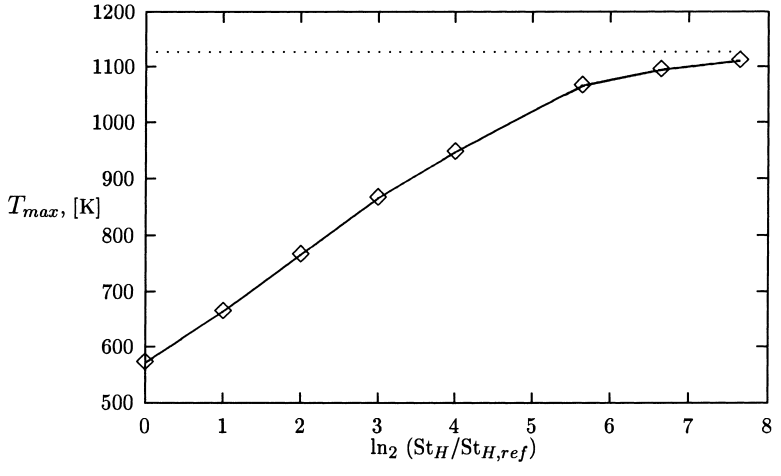

Fig. 11. Dependence of maximum temperature on heat transfer; St$_{H,ref}$=138.

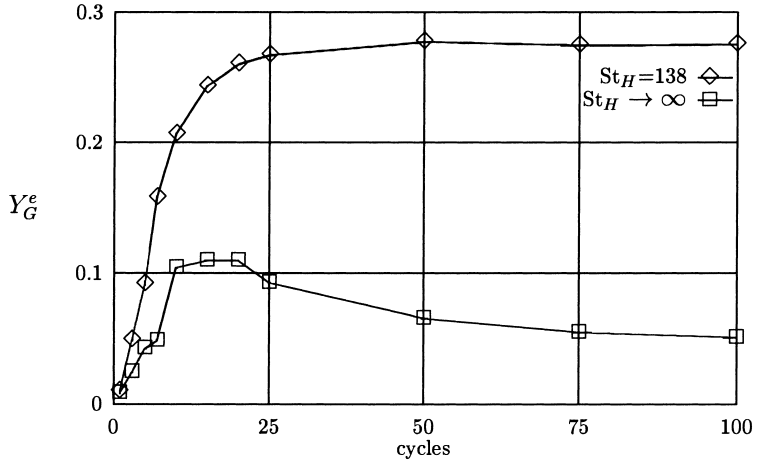

Fig. 12. Comparison of complete and simplified model prediction (St_H=138).

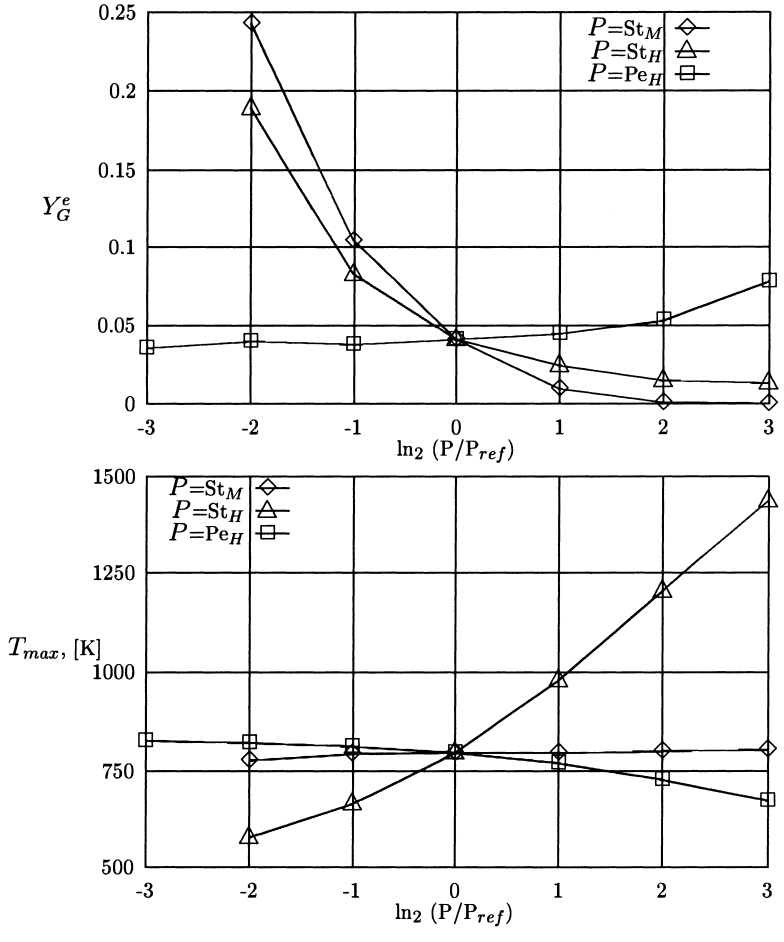

Fig. 13. Sensitivity analysis at ΔT_{ad}=30 K: residual concentration and maximum temperature.

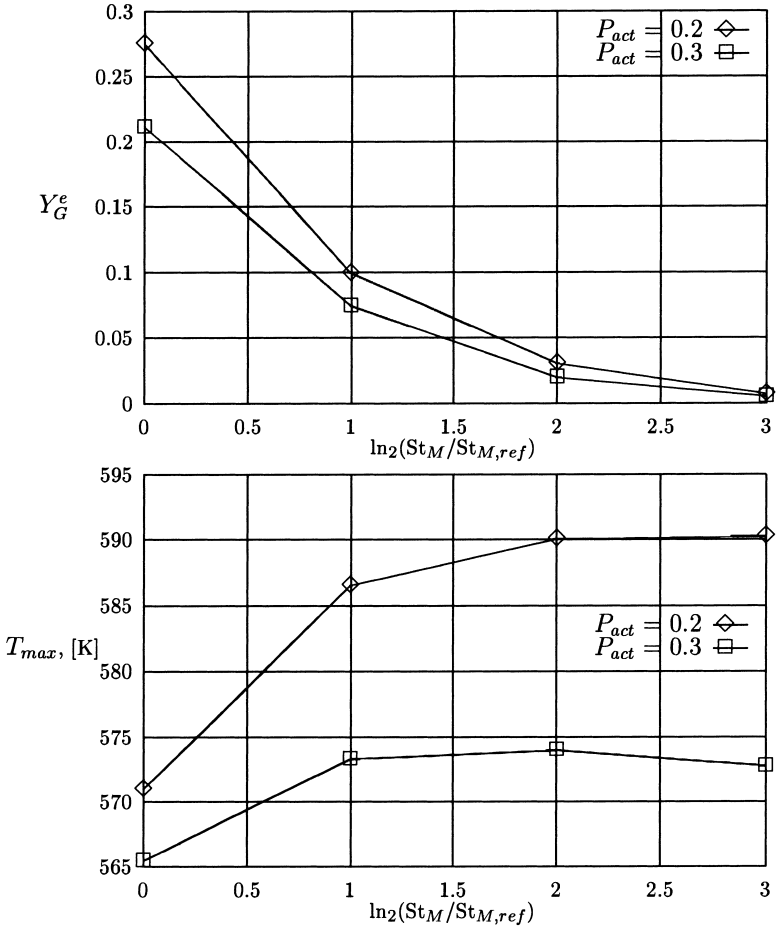

Fig. 14. Effect of St_M on residual concentration and maximum temperature for different catalyst lengths; ΔT_{ad}=10 K.

concentrations and also of gas flow rate, but conversion depends on setpoint and thus on preheat temperature.

Sensitivity analysis has evidenced that gas–solid heat and mass transfer are the most important parameters in determining final conversion. Maximum temperature is very sensitive to heat transfer, which cannot be considered as infinitely fast despite small temperature gradients between gas and solid. These dependencies are somewhat less pronounced at higher load.

6. Notation

a	specific interfacial area (m^{-1})
c	concentration (mol m^{-3})
c_P	heat capacity (J kg^{-1} K^{-1})
D_{eff}	dispersion coefficient (m^2 s^{-1})
d_P	particle diameter (m)
d_R	reactor diameter (m)
E_A	activation energy (J mol^{-1})
ΔH	heat of reaction (J mol^{-1})
h_t	gas–solid heat transfer coefficient (J m^{-2} K^{-1} s^{-1})
k_1	reaction rate constant (first order) (s^{-1})
k_∞	frequency factor (s^{-1})
k_{eff}	effective heat dispersion coefficient (J m^{-1} s^{-1} K^{-1})
k_G	mass transfer coefficient (m s^{-1})
L	reactor length (m)
M	molecular mass of gas phase (kg mol^{-1})
P	parameter (in sensitivity analysis)

P_{act} catalytically active portion (dimensionless)
p pressure (Pa)
R universal gas constant (J mol^{-1} K^{-1})
r rate of reaction (mol m^{-3} s^{-1})
s normalized time coordinate (dimensionless)
T temperature (K)
ΔT_{ad} adiabatic temperature rise (K)
t time (s)
u superficial velocity (m s^{-1})
v interstitial velocity (m s^{-1})
x axial space coordinate (m)
Y normalized molar fraction (dimensionless)
y molar fraction (dimensionless)
z normalized axial coordinate (dimensionless)

Greek letters

ϵ void fraction (dimensionless)
η conversion (dimensionless)
λ conductivity (J m^{-1} s^{-1} K^{-1})
ρ density (kg m^{-3})
τ dimensionless temperature

Subscripts

cat catalytic
eff effective
G gas phase
max maximum
ref reference value of centre point
S solid phase or solid interface
0 inlet conditions

Superscripts

′ kinetic parameter based on mass of catalyst and partial pressure
e exit
f feed

Acknowledgements

This work has been financially supported by the Italian National Research Council (CNR – Progetto Strategico). Support from the European Community in the form of a HCM Fellowship given to one of the authors (MB) is also gratefully acknowledged.

References

[1] J. Balmer, E.D. Gilles, Chem.-Ing.-Tech. 61 (1989) 632.
[2] G. Eigenberger, U. Nieken, Int. Chem. Eng. 34 (1994) 4.
[3] G.K. Boreskov, Y.Sh. Matros, Catal. Rev.-Sci. Eng. 25 (1983) 551.
[4] Y.Sh. Matros, Unsteady Processes in Catalytic Reactors, Elsevier, Amsterdam, 1985.
[5] Y.Sh. Matros, G.A. Bunimovich, Catal. Rev.-Sci. Eng. 38 (1996) 1.
[6] U. Nieken, G. Kolios, G. Eigenberger, Catal. Today 20 (1994) 335.
[7] Y.Sh. Matros, A.S. Noskov, V.A. Chumachenko, Chem. Eng. Process. 32 (1993) 89.
[8] J. Chaouki, C. Guy, C. Sapundzhiev, D. Kusohorsky, D. Klavna, Ind. Eng. Chem. Res. 33 (1994) 2957.
[9] B. van de Beld, R.A. Borman, O.R. Derkx, B.A.A. van Woezik, K.R. Westerterp, Ind. Eng. Chem. Res. 33 (1994) 2946.
[10] H. Züfle, Th. Turek, Th. Hahn, Behaviour of a fixed-bed reactor with periodic flow reversal, in: G. Centi et al. (Eds.), Environmental Catalysis, SCI, Rome, 1995, 659.
[11] H. Züfle, Th. Turek, Th. Hahn, Chem.-Ing.-Tech. 67 (1995) 1008.
[12] C. Sapundzhiev, J. Chouki, C. Guy, D. Klavna, Chem. Eng. Commun. 125 (1993) 171.
[13] B. Young, D. Hildebrandt, D. Glasser, Chem. Eng. Sci. 47 (1992) 1825.
[14] L. van de Beld, Air purification by catalytic oxidation in an adiabatic packed bed reactor with periodic flow reversal, Ph.D. Thesis, Twente, 1995.
[15] G. Eigenberger, U. Nieken, Chem. Eng. Sci. 43 (1988) 2109.
[16] M.F. Edwards, J.F. Richardson, Chem. Eng. Sci. 23 (1968) 109.
[17] R. Bauer, Effektive radiale Wärmeleitfähigkeit gasdurchströmter Schüttungen mit Partikeln unterschiedlicher Form und Größenverteilung, VDI Forschungsheft 582 (1977).
[18] V. Gnielinski, Verfahrenstechnik 16 (1982) 36.
[19] M. Brinkman, A.A. Barresi, M. Vanni, G. Baldi, Low exothermal reactions in a network of nonstationary catalytic reactor. Relevance of Control Policy, submitted to AIChEJ.